Manuscript file with track changes

Soil suction and temperature measurements in a heavy haul railway formation

Rick Vandoorne[1,*], Petrus Johannes Gräbe[2], Gerhard Heymann[3]

Department of Civil Engineering, University of Pretoria, Pretoria, South Africa, 0002

Abstract

Transportation foundations around the world exist predominantly in an unsaturated state. Support for the adoption of unsaturated soil mechanics in routine geotechnical engineering is ever-increasing. However, the measurement and characterization of soil suction is a potentially significant barrier thereto. To this end, the efficacy of various measurement techniques was investigated, with the aim to characterize the temporal variation in soil suction and temperature within the formation layers of a heavy haul railway formation. Tensiometers, fixed-matrix soil-water matric potential sensors and capacitance-type volumetric water content sensors were installed within the formation layers of a railway track and monitored for a period of 18 months. The average suction measured over the observational period was 25.6, 12.7, 3.5 and 4.2 kPa for the special subballast, subballast and two subgrade layers respectively. Suctions reached a minimum of ≈ 0 kPa at the end of the rainfall season across all layers and reached a maximum, ranging between 10 and 60 kPa across all layers at the end of the dry season. Soil temperatures for the observational period varied between 10 and 22 °C and displayed seasonality in-phase with the monitored air temperatures. The special subballast layer (uppermost layer) showed the greatest variation in both suction and temperature and is the layer which experienced the greatest stress changes as a result of seasonal variations in rainfall and air temperature.

Keywords: railway formation, soil suction, soil temperature, in-situ measurement, field measurement, weather

1. Introduction

Pavement and railway foundations are typically constructed above the water table. Thus, the soil directly influenced by traffic loading exists predominantly in an unsaturated state. However, saturated soil mechanics

*Corresponding author

Email addresses: vandoorne.r@gmail.com (Rick Vandoorne), hannes.grabe@up.ac.za (Petrus Johannes Gräbe), gerhard.heymann@up.ac.za (Gerhard Heymann)

[1]https://orcid.org/0000-0002-5426-8569

[2]https://orcid.org/0000-0002-1338-6075

[3]https://orcid.org/0000-0002-2338-4073

principles are still mostly used as the basis for their design (Houston, 2019). The fundamental understanding of unsaturated soil behavior has progressed significantly in recent decades (Fredlund, 2019). This progress has lead several prominent figures in the field to advocate for the adoption of unsaturated soil mechanics in routine geotechnical engineering practice (Rahardjo et al., 2019; Houston, 2019; Lu, 2020). Furthermore, the important role of unsaturated soil mechanics in dealing with the effects of climate change on transportation infrastructure has become increasingly evident (Toll et al., 2012b).

Soil suction and temperature are known to affect the resilient modulus and plastic strain accumulation of soils in the foundations of transportation infrastructure (Khoury and Zaman, 2004; Ng and Zhou, 2014; Chu, 2020; Qian et al., 2021). Using cyclic triaxial and hollow cylinder apparatus tests, Blackmore et al. (2020) found that useful estimates of resilient modulus could be made from measurements of soil suction. Using box tests of a reconstructed railway formation in the laboratory, Schulz-Poblete et al. (2019) found that the rate of plastic strain accumulation under cyclic loading in railway formation materials was dependent on the suction and moisture state of the respective layers.

Resilient modulus and plastic strain accumulation form an important part of pavement and railway design and performance assessment (Brown, 1996; Li et al., 2016). Thus, the prevailing suction and temperature conditions influence the design and performance assessment of pavement and railway foundations. However, the suction and temperature need to be known in order to account for their effect on pavement and railway foundation performance. This requires field measurement of the temporal variation of suction and temperature within railway formation materials.

One of the largest barriers to the implementation of unsaturated soil mechanics is related to the accurate and reliable measurement of soil suction. These difficulties are compounded when the measurements are made in the field (Bulut and Leong, 2008). As a result, studies in the literature concerned with the field measurement of soil suction within the foundations of pavements and railways are very limited. Whilst a few studies have been undertaken to monitor seasonal suction variation within pavement subgrades (Puppala et al., 2011, 2012; McCartney and Khosravi, 2013), limited similar studies have been identified in the literature concerned with the in-situ measurement of suctions within railway formations (Van der Raadt et al., 1987; Cui et al., 2014).

Permanent strain accumulation, resilient modulus and shear strength are all important considerations for railway formation design life prediction and performance assessment. Numerous laboratory and numerical studies have shown the significant influence of suction in this context (Khoury and Zaman, 2004; Ng and Zhou, 2014; Schulz-Poblete et al., 2019; Chu, 2020; Blackmore et al., 2020; Qian et al., 2021; Xie et al., 2021). However, laboratory studies often apply arbitrary suctions during testing, which are not related in any practical way to measured suctions within railway formation materials. Thus, the long-term in-situ measurement of suction within railway formations is important to guide imposed suctions and validate findings from laboratory studies.

The objective of this study was to measure and characterize the temporal variation of soil suction and temperature within the formation layers of a heavy haul railway formation. The efficacy of different suction measurement techniques for in-situ suction measurement within these railway formation materials was also assessed. The characterization of the temporal variation in soil suction and temperature can link well with laboratory studies to determine the expected change in formation layer response to loading under the measured in-situ conditions.

2. Suction Measurement Techniques

A review of various suction measurement techniques was conducted in order to determine which techniques were best suited for field application within the anticipated suction range. Furthermore, previous studies were reviewed to determine the extent to which soil suction and temperature had previously been measured and characterized below transportation infrastructure specifically.

Total internal soil-water potential is divided into matric potential and osmotic potential (Gens, 2010). Osmotic potential is generally only significant in high plasticity clay soils, which can display semi-permeable membrane-like behavior (Leong and Abuel-Naga, 2018). Therefore, this study was concerned solely with matric soil-water potential or matric suction. The term matric suction as used herein is defined as the negative matric soil-water potential. As such, positive pore-water pressures are represented as negative matric suctions.

Soil suction can vary over several orders of magnitude. This complicates its measurement and no single technique or apparatus exists that accurately covers the entire suction range of 0 – 1 000 000 kPa (saturated to oven-dry). Several suction measurement techniques are summarized in Table 1. Suction measurement techniques can be divided into direct and indirect techniques. Indirect techniques may be further divided into primary and secondary techniques. Tensiometers are an example of a direct measurement technique as they measure the physical tensile stress of a liquid in equilibrium with the soil-water potential.

Primary indirect measurement techniques make a measurement of the soil-water energy state within the soil. Examples of devices using such techniques include the psychrometer and dew-point hygrometer. These devices make a measurement of the relative humidity or water vapor pressure in the air in equilibrium with a soil sample. The relative humidity is related to total soil suction through Kelvin's Law (Gens, 2010).

Secondary indirect measurement techniques make a measurement of the soil-water energy state within a secondary porous medium which must be in equilibrium with the soil-water potential of the surrounding soil (Bulut and Leong, 2008). The filter paper technique is the most commonly used secondary indirect technique, especially in the laboratory (Marinho and Oliveira, 2006; Marinho and da Silva Gomes, 2012; Kim et al., 2017). Numerous devices utilizing secondary indirect techniques have been developed, both for research purposes and for commercial use. Such devices include thermal conductivity sensors (Feng et al.,

2002), dielectric permittivity sensors (Malazian et al., 2011) and electrical conductivity sensors (Varble and Chávez, 2011). Zhang et al. (2017) developed a novel apparatus that utilizes time domain reflectometry to determine the dielectric permittivity of the porous medium, whilst also measuring the dielectric permittivity of the surrounding soil. These types devices are sometimes collectively referred to as porous block sensors or granular matrix sensors. The porous blocks are generally manufactured from gypsum or a proprietary granular matrix (fixed-matrix) (Tarantino et al., 2008). These sensors are similar in the fact that they rely on the measurement of the water content of a fixed-matrix porous medium. The means by which the water content is measured varies between the different sensors (thermal conductivity, dielectric permittivity and electrical conductivity).

Heavy haul railway formation materials are typically granular in nature with a clay content of less than 10 % by mass (Transnet Freight Rail, 2006). Granular materials do not gain significant strength in the high suction range because the degree of saturation becomes too small. Thus, the contribution of soil suction towards suction stress and effective stress diminishes in the high suction range (Lu and Likos, 2006). Therefore, the suction range of interest for railway formation materials is likely to be in the low range of 0 – 1 500 kPa. Suction measurement techniques with reasonable accuracy in this range were thus considered.

The filter paper, psychrometer and dew-point hygrometer techniques are not well suited for field use. The filter paper technique requires regular placement and retrieval of filter papers within the soil profile of interest. The filter paper technique will at best provide discrete measurements and will not be able to capture the effects of rainfall events. Psychrometric methods are sensitive to temperature changes and are not suited for measurements in the low suction range (Bulut and Leong, 2008). The dew-point hygrometer apparatus requires material to be sampled and placed in the chamber of the apparatus and is thus not feasible for continuous field monitoring. Furthermore, the dew-point hygrometer is not sufficiently accurate

Table 1: Suction measurement techniques and their applicable ranges

Technique/Apparatus	**Type**	**Total or matric**	**Range** kPa	**References**
Filter paper	Secondary	Both	0 – 100 000	Bulut et al. (2001); Likos and Lu (2002)
Psychrometer	Primary	Total	300 – 30 000	Bulut and Leong (2008)
High-capacity tensiometer	Direct	Matric	0 – 1 500	Ridley (1993); Take and Bolton (2003)
Conventional tensiometer	Direct	Matric	0 – 100	Fredlund and Rahardjo (1993)
FSP sensor	Secondary	Matric	9 – 100 000	Tripathy et al. (2016); Meter Group, Inc. (2017)
Dew-point hygrometer	Primary	Total	100 – 300 000	Leong et al. (2003);Meter Group, Inc. (2020)

in the low suction range (Leong et al., 2003). Conventional tensiometers were not considered for use in this study due to their limited suction range in combination with the unknown suction regime present within the formation layers.

Two of the reviewed measurement apparatuses were identified for use for the field measurement of matric suction within railway formations materials. These were the high-capacity tensiometer and a commercial fixed-matrix soil-water potential (FSP) sensor (Meter Group, Inc., 2017). These apparatuses are suited for the measurement of matric suction in the range of interest and are also deployable in the field.

2.1. High-capacity tensiometers

High-capacity tensiometers differ from conventional tensiometers in that they allow the measurement of water pressures below 0 kPa absolute. This is achieved through the use of a high air-entry ceramic to separate soil-air from the tensiometer-water and a robust saturation procedure which removes entrapped air from the tensiometer and minimizes potential nucleation sites at which cavitation can occur (Take and Bolton, 2003). Tensiometer saturation typically involves the application of a vacuum to an oven-dry tensiometer, followed by the introduction and subsequent pressurization of de-aired water at the ceramic face. This is referred to as the two-stage saturation procedure and is generally accepted as the best saturation procedure (Toll et al., 2013). Tarantino and Mongiovì (2001) have found that cycles of cavitation and re-pressurization tend to increase the subsequent cavitation pressures achieved. Tensiometers are usually calibrated in the positive gauge pressure range and the calibration extrapolated into the negative pressure range. This procedure has been verified by numerous studies (Ridley, 1993; Guan and Fredlund, 1997; Tarantino and Mongiovì, 2003).

Low-cost high-capacity tensiometers were developed at the University of Pretoria which routinely measure suctions up to 500 kPa (Jacobsz, 2018; Le Roux and Jacobsz, 2021). These tensiometers were manufactured in-house at the University of Pretoria and have a material cost of approximately 27 US$ each (based on 2017 prices). Jacobsz (2018) verified the extrapolation of the positive pressure calibration into the negative pressure range for these tensiometers. Le Roux and Jacobsz (2021) demonstrated the use of these tensiometers for the measurement of soil-water retention curves (SWRCs) using the continuous tensiometer technique (Lourenço et al., 2011). Schulz-Poblete et al. (2019) identified that the tensiometers used by Jacobsz (2018) and Le Roux and Jacobsz (2021) were sensitive to total stress applications. The total stress response was mitigated by Schulz-Poblete et al. (2019) using an aluminum casing. For the current study a similar tensiometer design was used except that the aluminium casing was replaced by a stainless steel casing.

Fig. 1 shows an illustrative cross-section of the tensiometers built and used in this study. A 1 500 kPa high air-entry ceramic was fixed onto the face of a commercial pressure sensor using cyanoacrylate glue. The pressure sensing element is contained within a protective silicone gel. A small space between the silicone gel and the ceramic acts as the water reservoir for the tensiometer. The water reservoir is approximately

10 mm^3 in size (Jacobsz, 2018). After soldering the wires to the sensor, the ceramic and sensor are epoxied into the stainless steel casing. The epoxy is allowed to dry for two weeks before first use.

2.2. Commercial FSP sensor

A commercial fixed-matrix soil-water matric potential (FSP) sensor was also used to measure matric suction in-situ. The FSP sensors costed 310 US$ each (based on 2017 prices). The FSP sensor is a secondary indirect matric suction measurement apparatus. The FSP sensor was investigated as a potential alternative to the use of tensiometers for field measurement of matric suction. The FSP sensors are not subject to cavitation and thus require minimal to no maintenance after installation. The FSP sensor specifications according to the manufacturer are shown in Table 2. In addition to matric suction, the FSP sensors also measure temperature using a thermistor located beneath the overmolding of the sensor.

The components of the FSP sensor are illustrated in Fig. 2. The sensor comprises two engineered ceramic disks with a fixed pore size distribution, sandwiched between two stainless steel screens with a printed circuit board in the center. The printed circuit board makes a measurement of the relative dielectric permittivity of the ceramic disks using the capacitance technique. The relative dielectric permittivity of a vacuum, the solid ceramic material and water are 1, 5 and 80 respectively (Meter Group, Inc., 2017). Therefore, the relative dielectric permittivity measured is strongly related to the water content of the ceramic disks. The manufacturer determines a calibration curve for the FSP sensor in terms of measured relative dielectric permittivity versus applied suction along a drying path using a pressure plate apparatus. This calibration curve is analogous to the water retention curve for the ceramic except that the actual water content is not known. This calibration is stored on the sensor by the manufacturer and is not editable by the end-user.

When the FSP sensor is placed in contact with soil, the ceramic matric suction and the soil matric suction equilibrate over time. Equilibration occurs via the physical transfer of soil-water to or from the

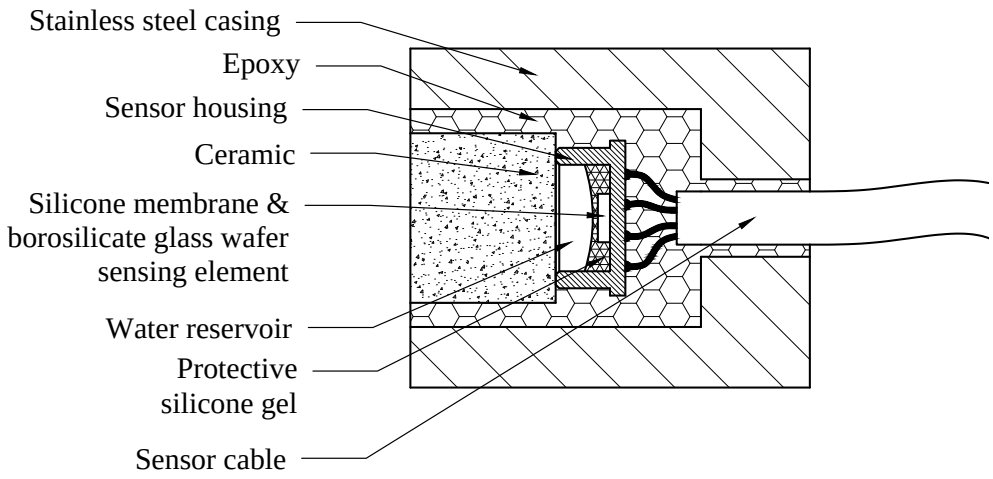

Figure 1: Cross-section of a low-cost high-capacity tensiometer indicating each of the components in their assembled position

ceramic disks. The rate of equilibration is dependent on the hydraulic conductivity of the surrounding soil, the hydraulic conductivity of the porous ceramic and the suction gradient between the soil and the ceramic. The degree of hydraulic continuity between the soil and the ceramic will significantly influence the equilibration rate. Once equilibrated, the water content in the ceramic disks is in equilibrium with the matric suction of the surrounding soil. A measurement of the relative dielectric permittivity of the disks is then made and used to back-calculate the matric suction in the disks by way of the calibration curve determined in the pressure plate apparatus.

Limited independent studies have been conducted regarding the accuracy of the FSP sensor. Various version of the sensor exist. The version used in this study was tested by Tripathy et al. (2016) and Karagoly et al. (2017) who compared suction measurements from the FSP sensor to suctions measured using the

Table 2: Manufacturer's specifications for the commercial FSP sensor used in this study (Meter Group, Inc., 2017)

	Matric suction†	**Temperature**
	kPa	°C
Range	9 – 100 000	-40 – 60
Resolution	0.1	0.1
Accuracy	± (10 % of reading + 2)‡	± 1

† Dissolved salts can move through the sensor's ceramic disk by diffusive or convective flow. Therefore, the osmotic potential of the water in the sensor ceramic and the osmotic potential of the soil-water are expected to be in equilibrium. Thus, the FSP sensor measures matric suction.

‡ This accuracy rating is only given for readings between 9 – 100 kPa.

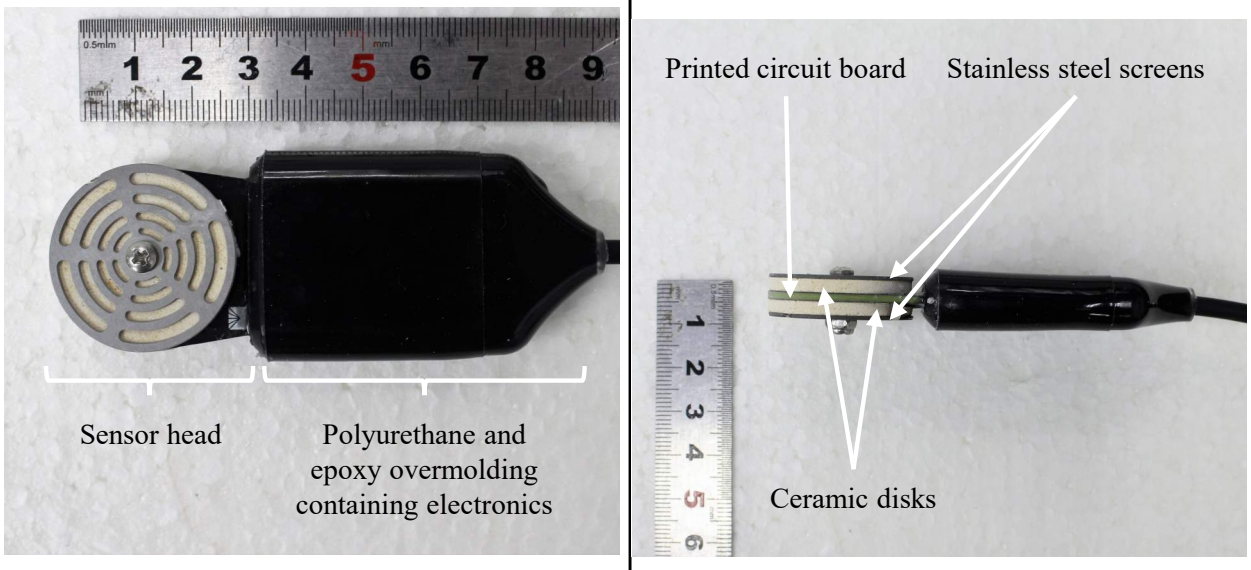

(a) Top view (b) Side view

Figure 2: Photographs showing components of the commercial FSP sensor used in this study

WP4C dew-point hygrometer (Meter Group, Inc., 2020). The materials used were a bentonite clay, kaolin clay, cement kiln dust and a quartz sand. The accuracy of the dew-point hygrometer as rated by the manufacturer was ± 50 kPa in the range 0 – 5 000 kPa. However, Leong et al. (2003) found that the potential error in a similar device was ± 150 kPa in the same range. Nonetheless, comparison of the FSP sensor readings and the dew-point hygrometer readings in the low suction range are not meaningful due to the limited accuracy of the dew-point hygrometer in this range. Furthermore, the dew-point hygrometer measures total suction whereas the FSP sensor measures matric suction. Thus, only soils with no osmotic suction can be compared. No significant conclusions can be drawn from these independent studies on the accuracy of the FSP sensors in the suction range 0 – 500 kPa. It was beyond the scope of this study to independently verify the accuracy of the FSP sensors.

The FSP sensor cannot measure positive pore-water pressure (negative suction) or suction changes in the range 0 – 9 kPa. This suction limit is due to the air-entry value of the ceramic disks, which is approximately 9 kPa. At suctions smaller than the air-entry value, the ceramic disks remain effectively saturated. Therefore, there is no detectable change in the ceramic disks' water content for suctions smaller than the 9 kPa air-entry value. The FSP sensors essentially measure the VWC of the ceramic disks and, therefore, if the water content of the ceramic disks does not change, a corresponding suction change cannot be determined. This is an inherent limitation of all porous block-type sensors.

3. Previous studies

Table 3 summarizes some studies that have attempted to measure soil suction below transportation infrastructure. The only studies identified that took place below a railway track were the studies by Van der Raadt et al. (1987) and Cui et al. (2014). Van der Raadt et al. (1987) used filter papers and AGWA-II thermal conductivity sensors to measure suction in-situ. Undisturbed samples were also taken and suctions measured in the laboratory using psychrometers. A 9 m long culvert was installed adjacent to the edge of the sleepers at several sites. Sensors were installed at depths of 0.15, 0.3, 0.6, 1.2, 2.4 and 3.6 m by drilling horizontally through the culvert into the soil profile underneath the track. The authors faced several problems related to the acquisition of the data from the AGWA-II sensors. The filter paper measurements also showed considerable scatter and the authors attribute this to uncertain filter paper contact conditions and potential artificial wetting of the filter papers due to condensation. The frequency and accuracy of the suction measurements meant that the variation of suction with rainfall events could not be identified. Furthermore, seasonality was only partially characterized due to uncertainties and errors in the suction measurements.

During an investigation into the behavior of interlayer soil (a mixed soil layer created by the interpenetration of ballast into the formation), Cui et al. (2014) installed suction probes at two different locations

at a railway site in France. The suction probes were installed at depths of 200, 300 and 500 mm below the bottom of the ballast layer at each of the two locations. Two more suction probes were installed at a third location adjacent to the track at depths of 300 and 500 mm. Each suction probe was located within its own specifically drilled borehole. The type of suction probes used are not mentioned. Therefore, the expected accuracy of the suction probes and the component of suction measured (matric or total) is unknown. It is also not clear whether the suction probes were installed within a bedding material to assist with hydraulic contact. The suction measured during the presented period did not increase beyond 10 kPa, which limits the ability to assess the high suction performance of the sensors used. The study concluded that the effect of the ballast layer limited evaporation below the railway track, resulting in the monitored suctions below the railway track not increasing beyond 2 kPa.

High-capacity tensiometers were successfully used in a trial embankment near Newcastle Upon-Tyne by Mendes et al. (2008), Toll et al. (2011) and Toll et al. (2012a). The novelty of their work lies in the design of a tensiometer probe locator that facilitated the easy installation and removal of tensiometers for maintenance. Unfortunately, suctions did not increase beyond 40 kPa during the observational period due to an abnormally wet period in the region. Thus, the high suction performance of the tensiometers in-situ could not be verified. A drift in the calibrated offset of the tensiometers was observed of approximately 5 kPa over a 2 year period. This suggests the need to check the zero readings of the tensiometers at regular intervals.

McCartney and Khosravi (2013) developed a novel method to monitor soil suction below pavements. A borehole was drilled and back-filled with alternating layers of silica flour and bentonite. Capacitance-type volumetric water content (VWC) sensors were installed within the silica flour layers. The bentonite layers served to mitigate piping or preferential flow of water through the silica flour. The measured VWC in-situ was then used to back-calculate the suction in the silica flour using a SWRC determined in the laboratory for the silica flour. The advantage of this method lies in the fact that VWC sensors in the past have generally proven more robust and reliable than suction measurement sensors for in-situ measurements. However, this method has several potential shortcomings. The accuracy of the method is influenced by:

- the void ratio of the silica flour which affects the SWRC expressed in terms of VWC
- hysteresis in the silica flour SWRC
- the slope in the area of the SWRC of concern
- the accuracy of the VWC determination

McCartney and Khosravi (2013) did not verify the suctions determined using any other devices or techniques. Their method of back-calculation is similar to the operating principle of the FSP sensor. However, the silica flour acts as the porous medium rather than the fixed-matrix porous ceramic. Therefore, there is

less control over the variability of the porous medium. Nonetheless, this novel technique is interesting as various materials could be used as the interfacing material to target suction measurements throughout the expected range.

There are several difficulties associated with the field measurement of matric suction. In their review of field measurement techniques, Harrison and Blight (2000) concluded that consistent, simple and reliable in-situ suction measurement techniques still alluded geotechnical engineers. With newer sensors this may potentially be overcome. However, records of long-term continuous in-situ suction measurement within the formation layers of a conventional ballasted railway track are still very limited.

Table 3: Summary of literature pertaining to the in-situ measurement of suction at transportation infrastructure

References	Location	№ sensors	Sensors used	Monitoring period	Suctions measured	Comments
Van der Raadt et al. (1987)	Railway shoulder	6	AGWA-II thermal conductivity sensors	≈ 4 months	60 – 275 kPa	• Sensors took 1–2 months to equilibrate • Readings taken manually • Filter paper measurements also taken, but showed considerable scatter • Local weather not monitored
Mendes et al. (2008); Toll et al. (2011); Toll et al. (2012a)	Test embankment	10†	Tensiometers	≈ 24 months	-15 – 40 kPa	• Data recording automated • Maintenance visit every 2 weeks • Shift in calibrated zero value suspected • Local weather monitored • Due to wet conditions, high suction performance could not be verified
Puppala et al. (2011); Puppala et al. (2012)	Pavement shoulder	4‡	FTC sensors	≈ 18 months	0 – 8 000 kPa	• Local weather not monitored • No redundancy in suction measurement • Readings taken manually • Only single sensor used at each site
McCartney and Khosravi (2013)	Pavement shoulder	5§	Capacitance-type VWC sensors¶	≈ 18 months	7 – 3 000 kPa	• VWC sensors were buried in silica flour and suction inferred from the SWRC of the silica flour • Only drying curve was considered • No attempt made at controlling in-situ dry density • Local weather not monitored
Cui et al. (2014)	Railway formation	8*	Unknown	≈ 10 months	0 – 10 kPa	• Local weather was monitored • No redundancy in suction measurement • Suction remained < 2 kPa below railway track

† Five sensors per hole.

‡ One sensor per site.

§ The exact number of sensors is not explicitly stated but data are presented for one of the seven sites showing five VWC sensors.

¶ Decagon 5TM sensors using the capacitance technique were used.

4. Field Installation

The site used in this study is located approximately 25 km southwest of Ermelo in Mpumalunga, South Africa. The formation was designed and constructed according to the Transnet Freight Rail (2006) 'Specification for Railway Earthworks S410'. The design axle load for the line is 26 tonne/axle. The line forms part of the Ermelo-Majuba Rail Project that was constructed to supply coal from the Mpumalunga coal fields to the Majuba Power Station. The site is located at chainage 21.5 km. To-date, however, there has been no operational traffic on the line. A modem was used to facilitate remote data retrieval as due to the location of the site, regular visits were not possible.

4.1. Site Selection and Layout

The safety of the sensors and logging equipment was paramount. Thus, a site adjacent to a relay room was selected which provided ample security. Fig. 3 shows a labeled aerial photograph of the site. A palisade fence and a 24-hour guard were present at the site. These security measures were necessary due to the nature of the equipment inside the relay room and the high risk of theft of copper cables, batteries and electronics.

The logging equipment was placed inside the relay room and all cabling was ducted through galvanized steel pipes installed below the ground surface. Only the weather monitoring equipment and the solar panel

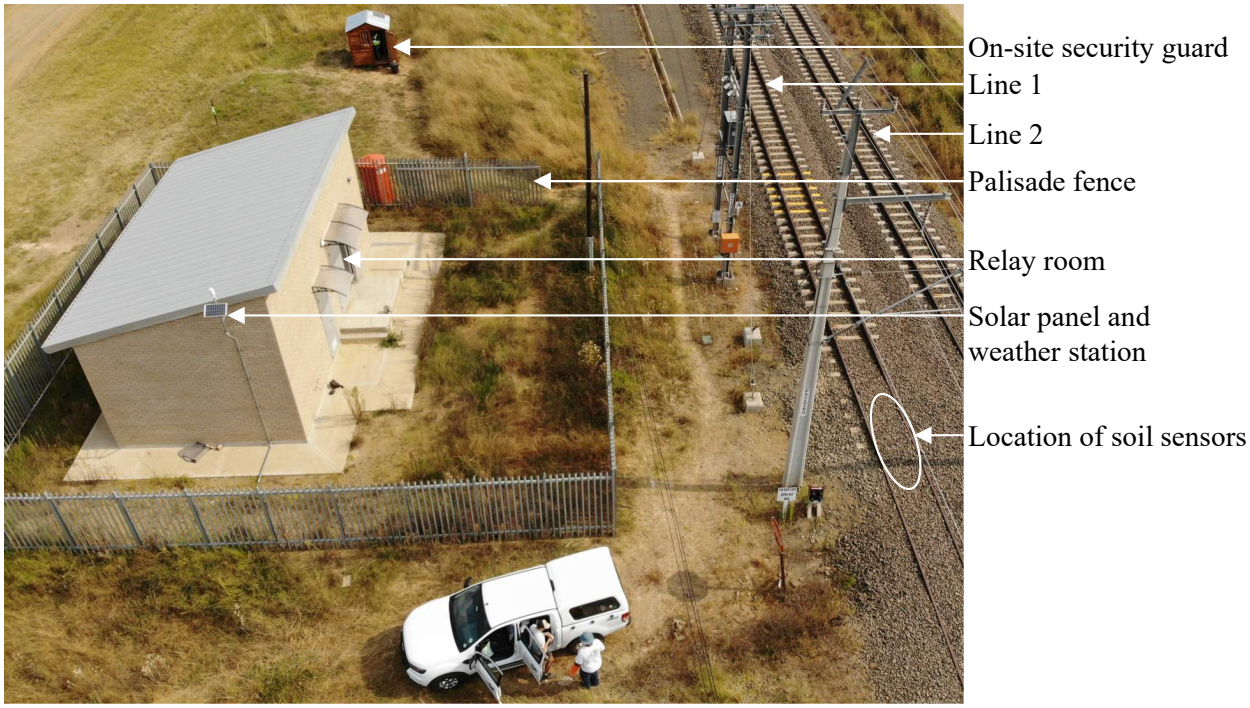

Figure 3: Aerial photograph of the instrumented site showing the general layout and security features

were located above ground. Power was provided at the site by a solar panel that charged a 12 V lead-acid battery via a solar charge controller. The battery was used to power the data logging hardware and modem. No alternate electricity was available at the site due to theft of the overhead traction lines which would normally supply electricity to the relay room.

4.2. Sensor Location and Installation

An access pit was excavated adjacent to the edge of the sleepers beneath the shoulder ballast to facilitate insertion, maintenance and removal of the sensors. A cross-section indicating the position of the access pit and sensor access pipes is shown in Fig. 4. The length of the holes was determined so that the sensors could be kept within eyeshot during the installation process. This was done to enable visual assurance of proper embedment of the sensors at the end of each hole. This limited the depth to which the sensors were installed and prevented the positioning of the sensors at the center line of the track.

Fig. 4 also shows the layer works at the site. The formation layer works consist of four layers namely the:

- special subballast (SSB) layer,
- subballast (SB) layer,
- subgrade A layer and
- subgrade B layer.

Material was sampled during excavation of the access pit for characterization. A summary of the specifications to which the layer works were constructed as well as the results of the characterization tests conducted

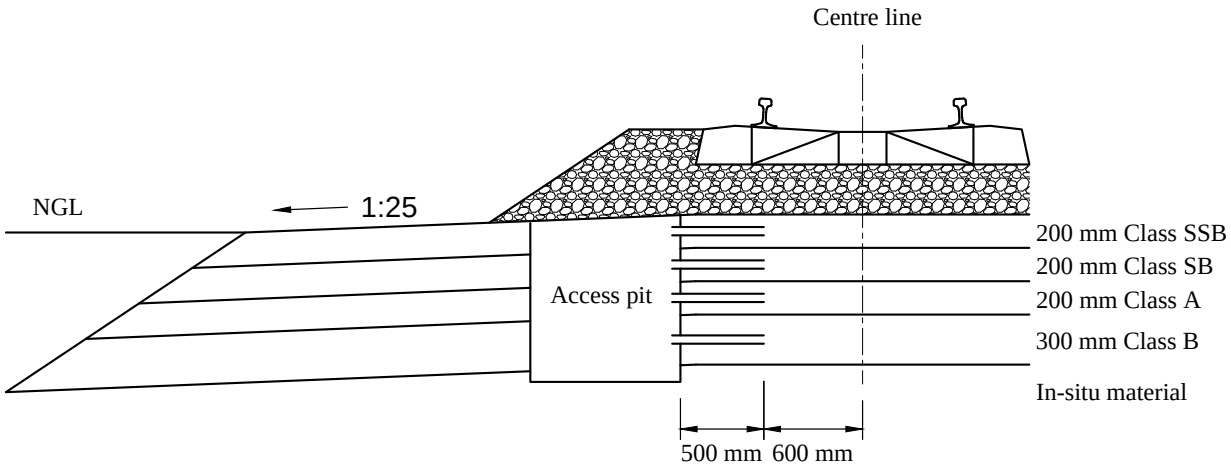

Figure 4: Transverse cross-section detailing the layer works, access pit location and sensor access pipe depths

on the sampled material are given in Table 5. Grading analyses, foundation indicator tests and compaction tests were conducted. The SSB and SB layer material was classified as a poorly graded gravel with silt and sand whilst the A and B layer material was classified as a clayey sand according to the unified soil classification system (USCS) (ASTM, 2018). The SSB and SB material was in fact material from the same borrow pit and therefore classify as the same material. The same is true for the A and B layer material. Therefore, only a single compaction test was conducted on the SSB/SB material and A/B material respectively. A photograph of the exposed layer works is shown in Fig. 5a. The Roman numerals I – IV in Fig. 5a identify the SSB, SB, A and B formation layers respectively.

The following four types of sensor installations were done:

- FSP sensors embedded within silica flour material
- tensiometers embedded within silica flour material

Table 5: Details of formation layer works at the site

Layer	**Mod. AASHTO MDD**	**Min. compaction of mod. AASHTO MDD**	**Thickness**	**Plasticity index**	**USCS**
	kg/m^3	%	mm	%	
SSB	2505	98	200	4	GP-GM
SB	2505	95	200	3	GP-GM
A	2139	95	200	9	SC
B	2139	93	300	9	SC

(a) (b)

Figure 5: Photos showing the construction of the soil sensor access pit: (a) excavated pit indicating the formation layers (b) complete installation

- VWC sensors embedded within parent material
- VWC water content sensors embedded within silica flour material

One of each of these types of installations was done within each formation layer for a total of 16 sensors. The respective locations of each sensor in the formation are shown in Fig. 6.

The silica flour was used to embed the FSP sensors and high-capacity tensiometers to assist with hydraulic continuity between the sensors and the soil-water of the formation layers. This is a common practice and a

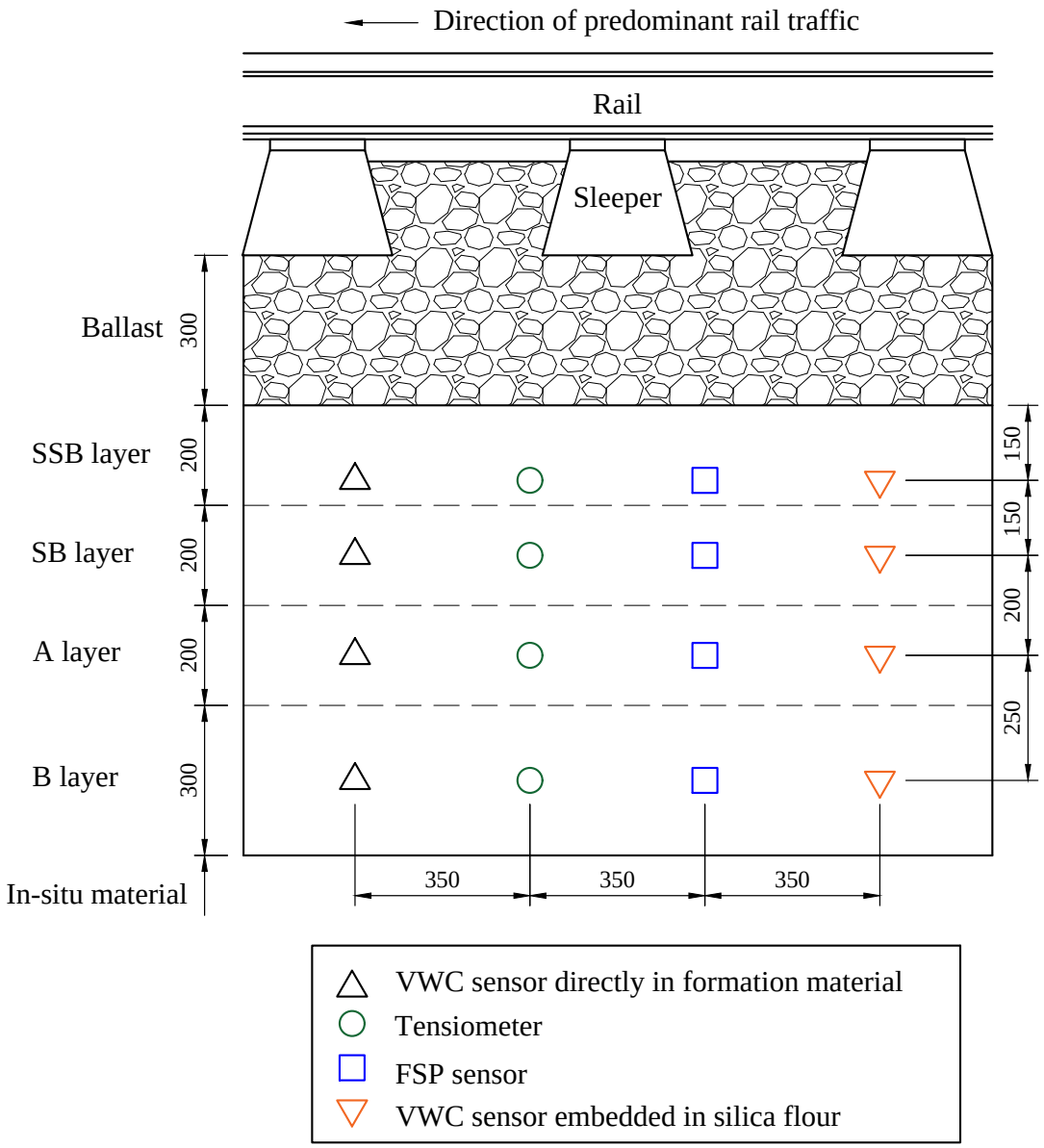

Figure 6: The relative location of each sensor installed in the formation

requirement of the bedding material is that the air entry value should at least be larger than the air-entry of the parent material (Nichol et al., 2003).

Capacitance-type VWC sensors were used (Meter Group, Inc., 2018). These sensors make a measurement of the capacitance of the surrounding medium which is related to the relative dielectric permittivity of the medium. The relative dielectric permittivity can be used to determine the VWC using the popular Topp (1980) equation. Several authors have shown that the accuracy of the VWC calculated from the measured dielectric permittivity may be improved if a soil-specific calibration is conducted. However, the accuracy of $\pm$ 3 % typically obtained when utilizing the Topp (1980) equation was deemed satisfactory for the present study (Matula et al., 2016; Parvin and Degré, 2016; Meter Group, Inc., 2018). The VWC sensors used also measure temperature in a similar fashion to the FSP sensors. Four VWC sensors were embedded within parent material and four VWC sensors within silica flour material. The VWC sensors within the parent material were aimed at providing an indication of the VWC of the formation layers. However, the VWC sensors could not be installed directly into the formation due to the granular nature of the material. Instead, a small amount of parent material finer than 2 mm was compacted down the sensor hole and the VWC sensor was embedded within this material. This process disturbed the dry density and void ratio of the material within which the sensor is embedded. Thus, the VWC sensors only provide an indication of VWC changes and should not be regarded as an absolute measurement.

Four more VWC sensors were embedded within a pocket of silica flour material. The aim of this installation type was to estimate the suction using the back estimation procedure as detailed and described earlier by McCartney and Khosravi (2013). Briefly, this relies on the measurement of the VWC of the silica flour in-situ which is in equilibrium with the suction of the surrounding soil. The VWC measured in the silica flour is then related to the silica flour suction by way of a laboratory measured SWRC. The dry density and void ratio of the silica flour were not controlled during installation as this was impractical.

Fig. 7 shows the general installation procedure followed for all the sensors installed in the formation. Using an electrically powered drill, holes 50 mm in diameter were drilled horizontally into the formation towards the center line of the track. The holes were $\approx$ 500 mm deep from the face of the excavated pit. Polyvinyl chloride (PVC) pipes of the same diameter were inserted into the holes to facilitate placement and retrieval of the sensors. An $\approx$ 150 mm gap was left between the end of the drilled hole and the PVC pipe (Fig. 7a). This is where the sensors were positioned after final installation. A large plastic bin was used as a manhole to facilitate future maintenance activities (Fig. 5b).

An $\approx$ 120 mm bedding layer of material was compacted down the hole using a hand operated compaction ram (Fig. 7b). As previously stated, the bedding material used was either sieved parent material or silica flour, depending on the sensor that was installed. Thereafter, the sensors were inserted using a specially manufactured probe locator into the compacted material. The probe locator was used to firmly press the sensor into the bedding material. Parent material or silica flour was then used to backfill the remaining space

behind the sensor in the PVC pipe. This material was compacted behind the sensor using the compaction ram to ensure good contact between the installed sensor and the surrounding soil. Each of the access pipes was sealed using an end cap and an adhesive polyurethane sealant to ensure water could not seep into the access pit from the formation layers or vice versa. A photograph of the access pit after complete installation of the sensors is shown in Fig. 5b.

The tensiometer installation differed from the other sensors somewhat. The tensiometer locator probe was left in place and sealed rather than the access pipe being back-filled over its entire length. This was done to facilitate easy retrieval if necessary. A screw was used to fix the tensiometer probe locator to the PVC access pipe to ensure that it did not move after installation and that adequate hydraulic contact was maintained. The tensiometer data was monitored during installation to ensure that the tensiometers did not cavitate.

Fig. 8 shows a photograph of the solar panel and weather monitoring equipment mounted to the northern wall of the relay room. An all-in-one weather station was installed at the site to monitor meteorological parameters including air temperature and rainfall amongst other parameters not presented herein. The rain gauge in the all-in-one weather station proved unreliable and prompted the installation of a separate tipping bucket rain gauge. Rainfall data from a South African Weather Service weather station located at Ermelo Airfield was used for dates on which erroneous rainfall data was recorded by the all-in-one weather station. There were only five instances of this during the observational period.

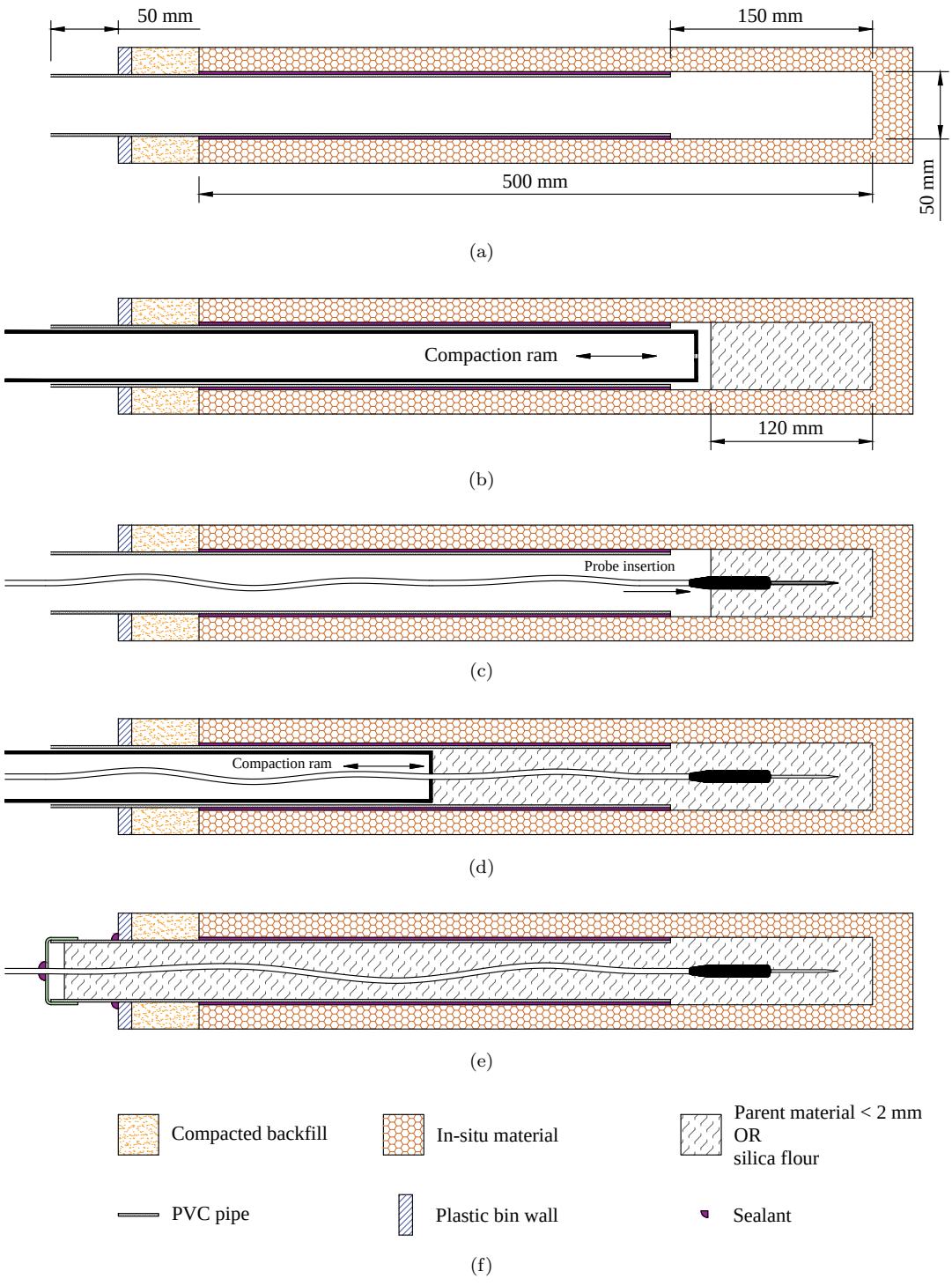

Figure 7: Schematics illustrating the installation of the sensors: (a) approximate depth to which the PVC pipes are inserted (b) parent material passing the 2 mm sieve or silica flour is compacted down the hole to a depth of ≈ 120 mm (c) the sensor is inserted into the compacted material using a probe locator until only the rear end of the overmolding is visible (d) the area behind the sensor is back-filled and compacted (e) the PVC pipe is capped and sealed (f) legend

Figure 8: Photo showing the mounted all-in-one weather station, tipping bucket rain gauge and solar panel

5. Results

The observational period is defined as 1 Aug. 2019 – 31 Dec. 2020. The initial installation was completed on 27 July 2019. Water damage at the site resulted in a data unavailability period for the soil sensor data from 26 Oct. 2019 – 27 Feb. 2020. This period corresponds to the summer months when most of the annual rainfall is expected in this region.

5.1. Suction

Fig. 9 shows the suctions measured by the tensiometers and FSP sensors over the full observational period. The tensiometer installed in the SSB layer showed fluctuations in phase with relative humidity and air temperature during the first three months and is, therefore, not shown for this period. This behavior is indicative of poor saturation or poor hydraulic contact and has previously been reported by Toll et al. (2011). All tensiometers were replaced on 27 Feb. 2020 during the repairs to the water damage at the site and appeared reliable from this date onward.

Evidence from the literature has shown that tensiometer measurements may show drift of ± 5 kPa during prolonged periods of use (Mendes et al., 2008). Therefore, tensiometer offsets were measured at the site in Dec. 2019 for the tensiometers installed on 27 July 2019. It was determined that the offsets remained within ± 2 kPa of those determined at initial installation. Tensiometer offsets after initial installation were not determined for the tensiometers installed on 27 Feb. 2020.

The FSP sensors were installed dry and took 1–2 months to equilibrate. The varying equilibration rates may be due to varying degrees of hydraulic contact between the FSP sensors and the silica flour within which they were embedded. Tripathy et al. (2016) showed that wetting the FSP sensors before installation could improve the equilibration time. After equilibration, the tensiometers and FSP sensors displayed similar suction trends. The only clear deviation in suction trends between the tensiometers and the FSP sensors occurred for the period 1 Oct. 2020 – 31 Dec. 2020 in the SB layer. The reason for this is not clear but may be due to poor tensiometer hydraulic contact or a delayed response of the FSP sensor to increasing suctions. Loss of adequate hydraulic contact may arise due to movement of the tensiometer ceramic face away from the silica four into which it was embedded. This movement may be caused by collapse settlement of the silica flour upon wetting or minor void ratio changes of the silica flour around the ceramic face of the tensiometer during repeated drying and wetting cycles. The lowest suction that the FSP sensors can measure is limited by the air-entry of the ceramic disks to $\approx$ 9 kPa. For this reason, the suction trends between the tensiometers and FSP sensors cannot be accurately compared for suctions less than 9 kPa. This lower suction limit of the FSP sensors is a severe limitation in near saturated conditions as were experienced at the monitored site.

From Fig. 9 it is also evident that the SSB and SB layer suctions varied more than the A and B layer suctions. The suctions in the A and B layers remained near 0 kPa for the majority of the observational period. This suggests that there was not adequate drainage at the site to sustain significant levels of suction for significant periods of time, particularly in the A and B layers. There was no formal drainage at the site and during one of the site visits the water table was observed at the level of the formation layers.

Fig. 10 shows a direct comparison between the suctions measured by the tensiometers and the suctions measured by the FSP sensors in the SSB and SB layers. The data for these layers are shown as the suction in these layers displayed significantly more variation over the observational period than the suctions in the A and B layers. Data for the period 1 Mar. 2020 – 31 Dec. 2020 are shown as reliable tensiometer data for the SSB layer were unavailable before this period. The largest differences occurred in Dec. 2020 for the SB layer, during which the suction measured by the tensiometer increased to $\approx$ 30 kPa but the suction measured by the FSP sensor remained at $\approx$ 9 kPa. If one excludes the deviation in trend shown in the SB layer for Nov. – Dec. 2020, Fig. 10 shows that the differences in measured suctions between the tensiometers and FSP sensors remained within a $\pm$ 10 kPa band. This difference is significant at the low suction levels dominating at the monitored site. Due to the fact that the tensiometers could measure suctions below 9 kPa, their data are presented and discussed further herein with regard to seasonal trends.

Figs 11–14 show the suctions measured by the tensiometers and FSP sensors in the SSB, SB, A and B layers respectively over the full observational period. The average monthly suction and total average suction for the observational period are also shown in each figure for each respective layer. The daily rainfall data are also superimposed on each figure.

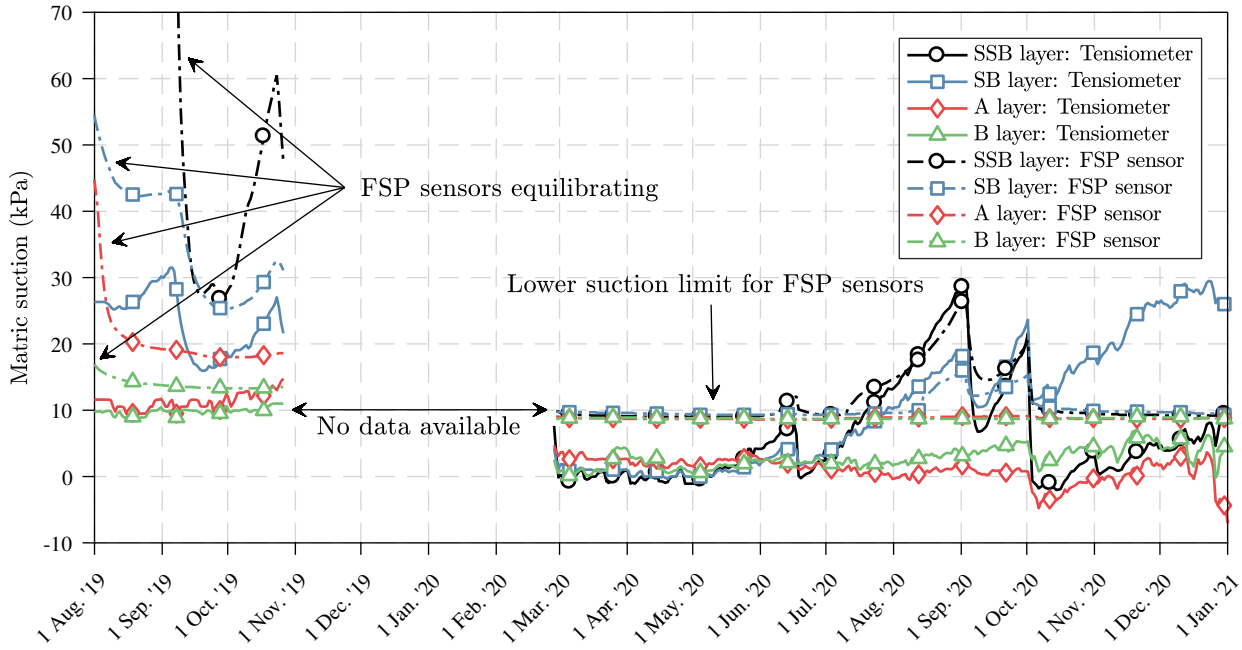

Figure 9: Formation layer suction measured by the tensiometers and FSP sensors over the observational period

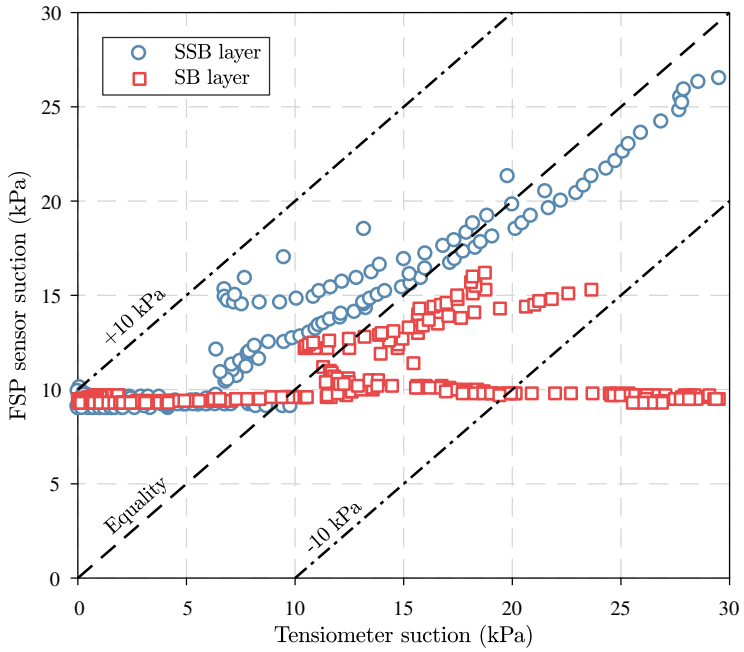

Figure 10: Direct comparison between FSP and tensiometer measured suctions in SSB and SB layers for the period 1 Mar. 2020 – 31 Dec. 2020

The SSB layer shows the greatest variation in suction over the observational period. The SB layer shows a similar trend in suction variation to the SSB layer. However, the range of suction variation is subdued in comparison to the SSB layer. This is expected as the SSB layer is closer to the surface and is thus most affected by rainfall infiltration. The maximum suction recorded in the SSB layer was 30 kPa in Sept. 2020. However, it is suspected that a higher suction would have been recorded in Oct. 2019 if the tensiometer was functioning correctly on this date. This was assessed using the suction measured by the FSP sensor in the SSB layer during this period. According to the FSP sensor, the suction approached 60 kPa in the SSB layer in Oct. 2019. The maximum suction recorded in the SB layer was 32 kPa in Sept. 2019.

Both the SSB and SB layer suctions show an inverse relationship with rainfall. Suctions in these layers were observed to dissipate completely after the rainfall in the wet summer months. In the drier winter months that followed, the suctions increased steadily until the next summer rainfall period started. Comparison of the average monthly suction and the daily rainfall illustrate the relationship between rainfall and suction within the SSB and SB layers clearly.

Suction variation in the A and B layers was minimal (Figs 13 and 14). Similar suctions were recorded in both the A and B layers. A fairly constant suction of $\approx$ 10 kPa was measured before the wet summer months started. By the end of the summer months, the suction in both the A and B layers had dissipated to between 0 and 5 kPa. The suction in the A layer for Oct. 2020 and part of Dec. 2020 was negative, indicating positive pore-water pressure. However, the B layer suction did not indicate positive pore-water pressure for the same period. This is contradictory as positive pore-water pressures are indicative of a water table which means that the B layer should also have registered a positive pore-water pressure. This may be indicative of an offset error that had developed between the A and B layer tensiometers. This was not confirmed and would require another assessment of the tensiometer offsets.

Further indication of potential drift in the tensiometer measurements can be seen when comparing the suction data for the period 1 Oct. 2020 to 1 Jan. 2021 for the SSB and SB layers (Figs 11 and 12). During this period the suction measured by the tensiometers in these layers appears to increase gradually despite frequent rainfall events. Maximum and minimum daily air temperatures (Fig. 17) had significantly increased during this period as compared to the previous months, which would have significantly increase evaporation rates from the surface. This could lead to excess water extraction and an increase in suction despite rainfall events. However, the suction measured by the FSP sensors did not increase with the suctions measured by the tensiometers in these layers. This supports the theory that the tensiometers in the SSB and SB layers may have drifted in the last three months of the full observational period. Similar tensiometer drift has been reported by Mendes et al. (2008).

Fig. 15 shows soil suction profiles at four different dates during the observational period. The figure clearly demonstrates that soil suction fluctuates more in the shallow layers of the formation than the deeper layers. Thus, suction variation appears to be related to the depth of the soil below the surface. The suction

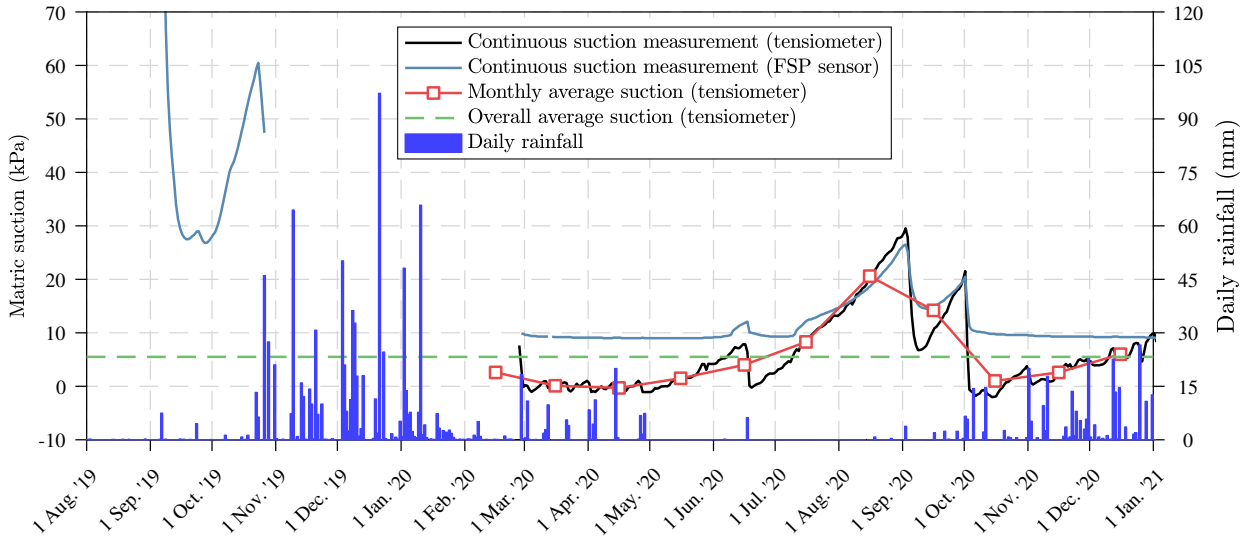

Figure 11: Temporal variation of suction in the SSB layer with rainfall

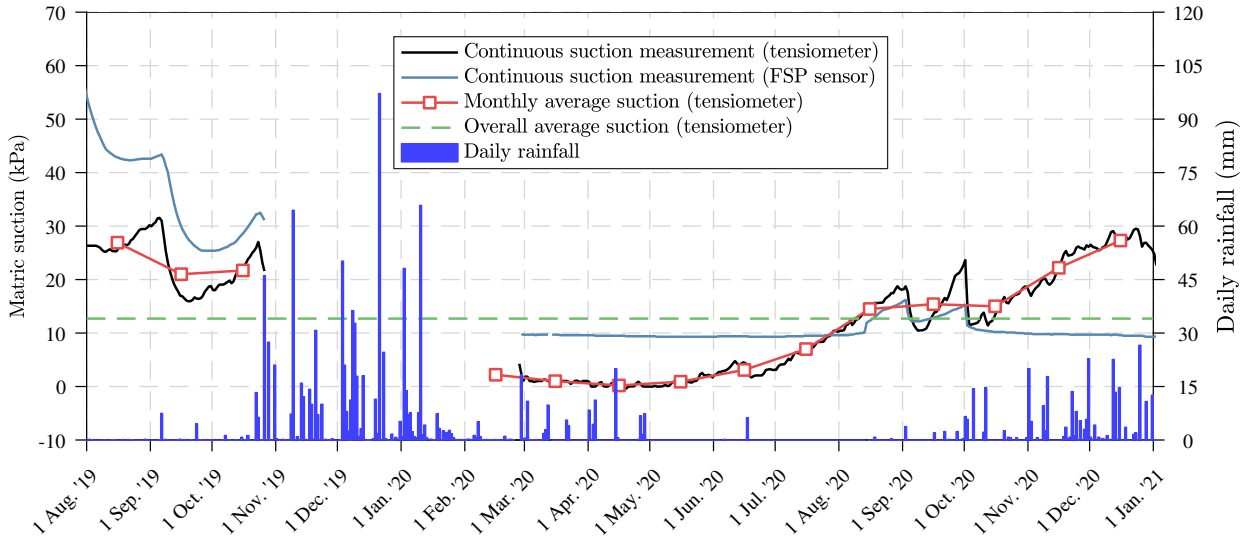

Figure 12: Temporal variation of suction in the SB layer with rainfall

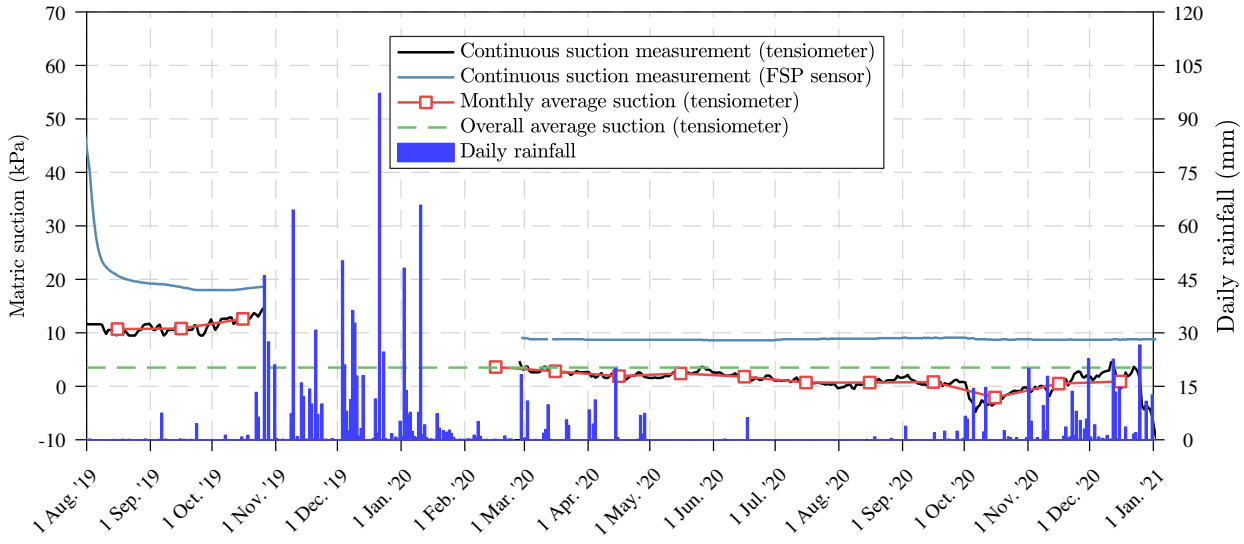

Figure 13: Temporal variation of suction in the A layer with rainfall

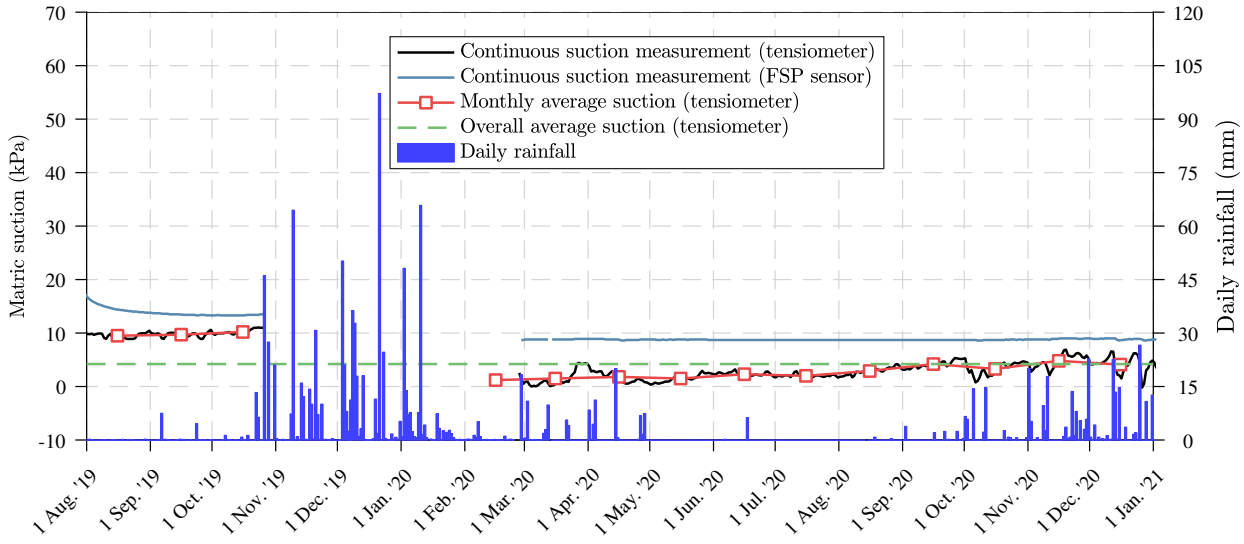

Figure 14: Temporal variation of suction in the B layer with rainfall

range observed in Fig. 15 in the SSB layer is 0 – 60 kPa, whilst the suction range observed in the B layer is 0 – 12 kPa. The suction profiles for 28 Sept. 2019 and 23 Oct. 2019 correspond to periods with minimal to no rainfall, where evaporation from the surface dominates. The suction profile for 4 May. 2020 shows that the suction in all the formation layers was effectively zero after the summer rainfall months. The suction profile for 4 Sept. 2020 shows a gradual recovery of the suctions in the uppermost layers due to an extended period with no rainfall accompanied by evaporation from the surface.

The average suctions in the SSB, SB, A and B layers over the observational period were 5.5, 12.7, 3.5 and 4.2 kPa respectively as measured by the tensiometers. The average suctions as measured by the FSP sensors were 25.6, 15.6, 11.2 and 9.8 kPa. The average suction measured by the tensiometers for the SSB layer is skewed due to the lack of data in the first few months when the highest suctions occurred. Thus, the FSP average suction in the SSB layer is more representative of the true average suction in the SSB layer. The average suctions over the observational period indicate that the suction in the upper most layer is the highest and a decrease is observed with an increase in depth. This is, however, only true on average.

5.2. Water Content

Fig. 16 shows the VWC measured within the formation layer material over the observational period. These VWC sensors were embedded within the parent material passing the 2 mm sieve, which was subsequently re-compacted down the access hole. The measured weekly rainfall is superimposed over the VWC data. The VWC sensor in the SSB layer malfunctioned on 1 Mar. 2020 and is thus not shown in Fig. 16. The dielectric permittivity measured by the VWC sensors was converted to VWC using the Topp (1980) equation.

VWC is observed to increase with depth. This result is expected for a soil profile which is at equilibrium with a water table. The measured VWC did not fluctuate in the same manner as the measured suctions. The B layer showed the most fluctuation in VWC, however, the B layer suctions only showed minor variations in suction. The VWC in the SB layer showed minor variation. The peaks in VWC in the B layer are believed to correspond to a rising and lowering water table. This would indicate that the water table is near the surface during the rainfall months and corroborates the low suction readings obtained at the site by the tensiometers and FSP sensors. The measured VWC was not as sensitive to rainfall events as the measured suctions. This is potentially due to air gaps around the sensor prongs.

The VWC sensors which were embedded within the silica flour material did not perform as expected. The VWC measured by these sensors did not correspond to the suction or VWC hierarchy measured by the other sensors. The data from the silica flour VWC sensors are not shown herein as the data was clearly unrepresentative of the conditions within the layers as measured by the other sensors. It is believed that many of the silica flour VWC sensors suffered from inadequate soil contact. The silica flour material does not compact well due to its particle size distribution. Furthermore, erosion and piping was observed in the

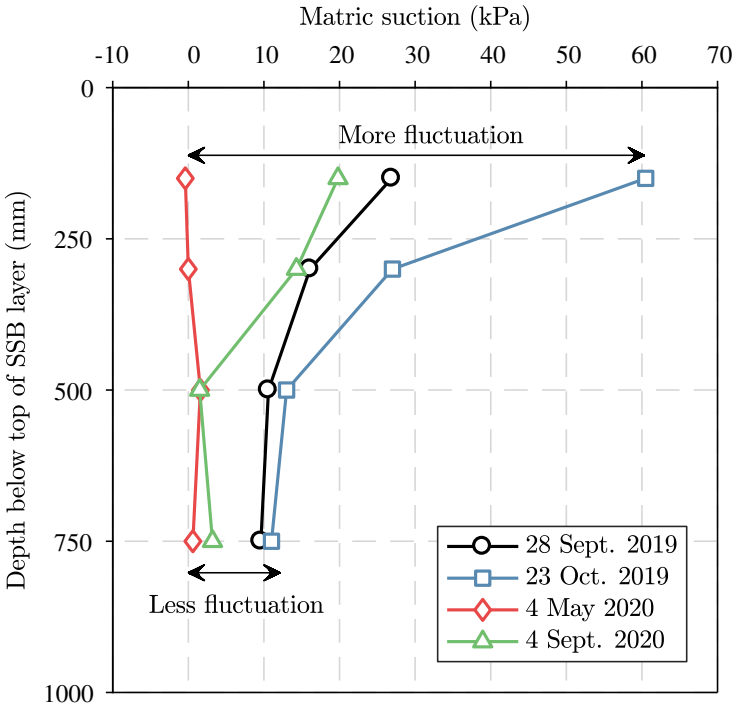

Figure 15: Suction profiles within the formation layers at different times

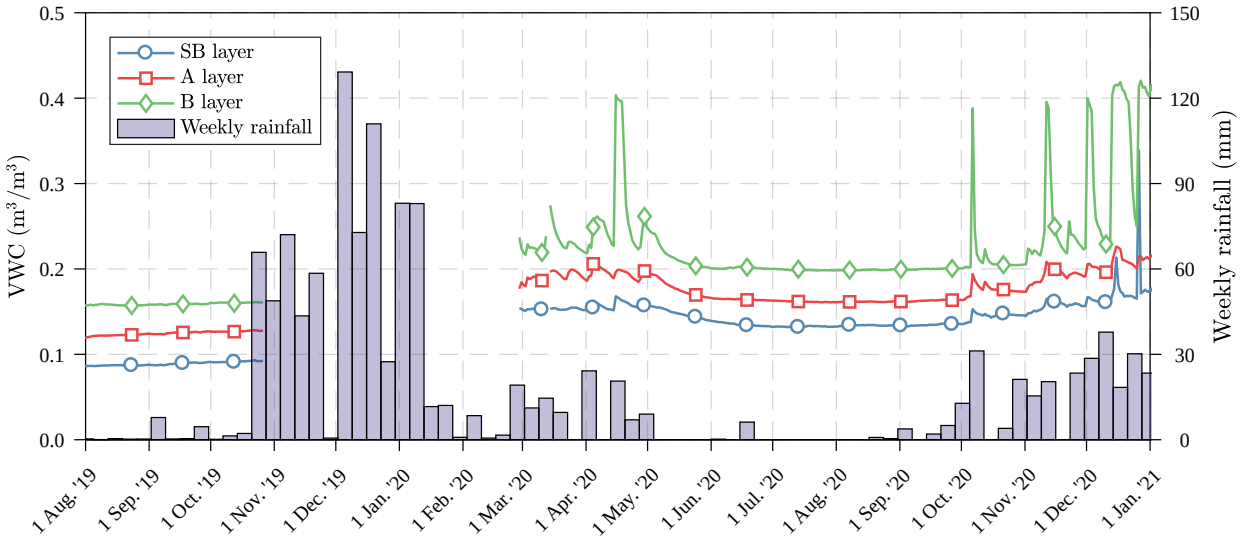

Figure 16: Temporal variation of VWC in the formation material with rainfall during the observational period

silica flour material for the holes within which these sensors were located. It is believed that this may have created air pockets around some of the sensors which were registered as an unreasonably low VWC. Due to the poor data recorded by the VWC sensors in the silica flour, the efficacy of the back-calculation technique used by McCartney and Khosravi (2013) could not be assessed herein. It is felt that better results may be obtainable if the VWC sensors are installed in a vertical hole rather than a horizontal hole where erosion and piping of the silica flour material can occur.

5.3. Temperature

Fig. 17 shows the daily maximum and minimum air temperature recorded by the all-in-one weather station over the observational period. A seasonal trend is evident. Daily maximum and minimum air temperature fluctuate in a cyclic manner with higher minimum and maximum air temperatures occurring in the summer months (Dec. – Feb.) as opposed to the winter months (June – Aug.). It is worth noting that the difference between the daily maximum and minimum air temperature increases in the summer months and decreases in the winter months.

Good agreement was observed between the FSP and VWC sensor temperature data within each layer. Thus, the average of the three sensors in each layer was used as the representative temperature value for that layer. Fig. 18 shows the average formation layer temperature for each layer over the observational period. Seasonality is evident, with minimum soil temperatures approaching 10 °C in July and maximum soil temperatures approaching 22 °C at the end of Dec. The true maximum soil temperature may be higher than 22 °C due to the data unavailability period, which corresponded with the hot summer months. The seasonal variation of $\approx$ 12 °C is expected to have a small, yet measurable effect on the formation layer response to cyclic loading by trains. This has been shown in laboratory studies (Zhou and Ng, 2016).

The range in formation layer temperatures at a given time is larger during the winter months than the summer months. The cooler air temperatures in the winter months appear to drive the SSB and SB layers' temperatures below that of the A and B layers. However, in the summer months, the SSB and SB layers' temperatures are in general equal to or greater than the A and B layers' temperatures. The summer rainfall appears to drive down the SSB and SB layers' temperatures occasionally which results in a smaller range of formation layer temperatures in the summer months. The minimum soil temperature recorded during the observational period of 10 °C indicates that freeze thaw phenomena are likely not of concern in this region of South Africa.

Fig. 19 shows soil temperature profiles at four different dates during the observational period. The formation layer temperatures were all similar on 8 Oct. 2020. In the absence of any rainfall, the formation layer temperatures increased from 8 Oct. – 10 Oct. 2020. On 11 Oct. 2020 a rainfall event of 16.8 mm occurred. This rainfall event along with subdued air temperatures resulted in a decrease in soil layer temperature as seen by the profile dated 13 Oct. 2020. The temperature decrease is inversely related to

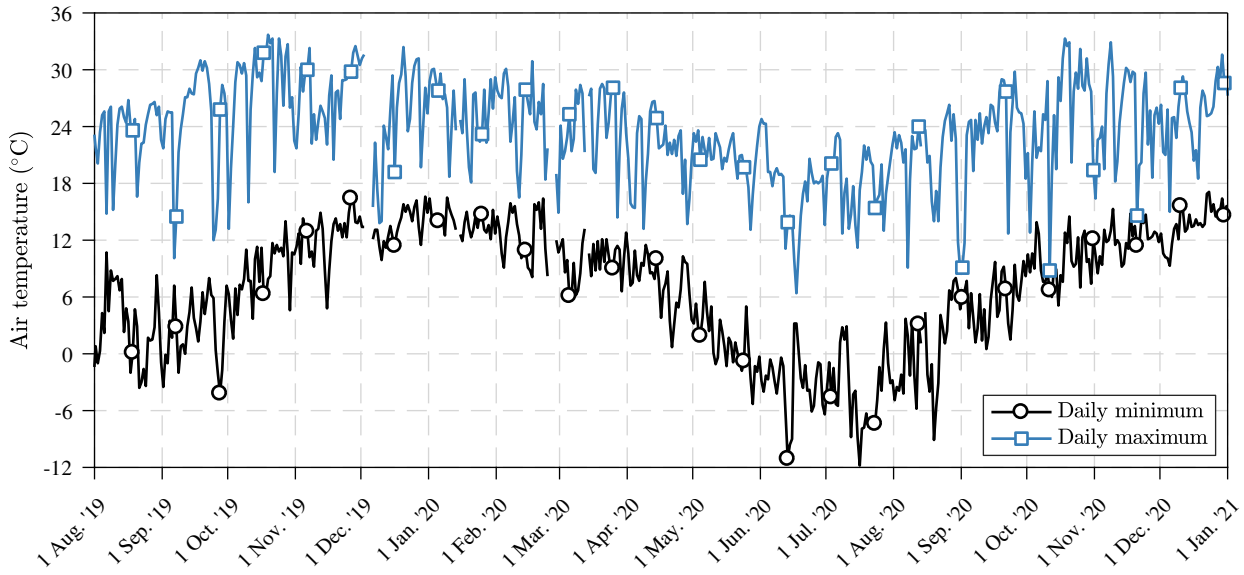

Figure 17: Daily minimum and maximum air temperatures during the observational period

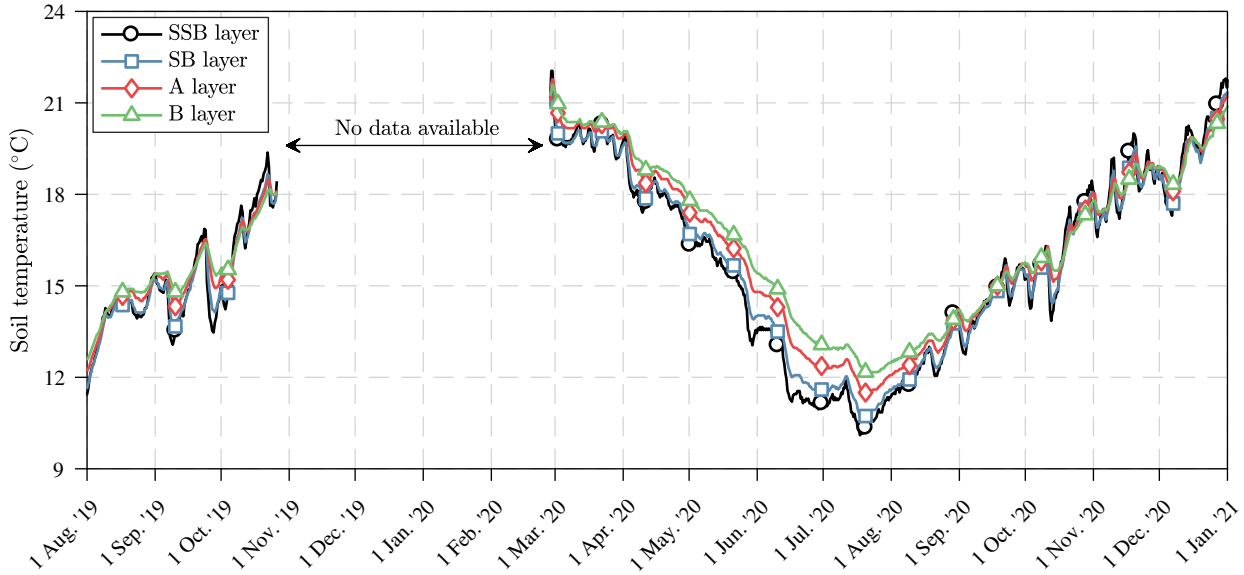

Figure 18: Temporal variation of formation layer temperature during the observational period

the depth of the layer. The profile dated 20 Oct. 2020 corresponds to a time seven days after the rainfall event of 16.8 mm. The temperature profile shows that the formation layers' temperatures all increased to beyond their pre-rainfall temperature within seven days. Fig. 19 also illustrates that the relative magnitude of the temperature changes observed decreases with an increase in depth. The absolute range of temperature changes observed at a given depth, however, will be influenced by the duration of the observation period (An et al., 2017).

6. Conclusions

High-capacity tensiometers and commercial fixed-matrix soil-water matric potential (FSP) sensors were used to monitor the temporal variation of soil suction within the formation layers of a heavy haul railway. The commercial FSP sensor was investigated as a potential alternative to the use of tensiometers for field suction measurement. Volumetric water content (VWC) was also monitored using a capacitance-type VWC sensor. The FSP and VWC sensors were also used to monitor soil layer temperature. Air temperature and rainfall were monitored at the site. One of each type of soil sensor was placed within each of the four formation layers namely the special subballast (SSB), subballast (SB), A and B layers.

Reasonable agreement was found between the suction trends measured by the FSP sensors and the tensiometers. In terms of absolute accuracy, the FSP sensor readings remained within $\pm$ 10 kPa of the tensiometers readings throughout most of the 18-month observational period. The tensiometers showed some drift in their offsets, which was confirmed to be within $\pm$ 2 kPa over a 4-month period. Drift over longer periods was not verified. The FSP sensors required no maintenance during the observational period whilst the tensiometers were replaced approximately midway through the observational period as a precautionary measure and to rectify a problematic tensiometer in the SSB layer. The lower suction limit of $\approx$ 9 kPa was found to be a major limitation of the FSP sensors due to the low suction conditions at the monitored site.

The average suction measured over the observational period was 25.6, 12.7, 3.5 and 4.2 kPa for the SSB, SB, A and B layers respectively. The suctions in the SSB and SB layers responded to individual rainfall events and showed appreciable seasonal variation. The suctions in the SSB layer showed the greater variation with rainfall events between these two layers. The suctions in the A and B layers did not show any apparent variation with individual rainfall events and also showed minimal seasonal change. Suctions reached a minimum of $\approx$ 0 kPa in Mar. 2020 (the end of the rainfall season) across all layers and reached a maximum, ranging between 10 and 60 kPa across all layers in Oct. 2019 (the end of the dry season).

Soil temperatures displayed seasonality that was in-phase with the observed seasonality in the daily maximum and minimum air temperature measurements. Soil temperatures for the observational period varied between 10 and 22 °C. A wider range in soil layer temperature was observed between the formation layers during the winter months when compared to the summer months. Rainfall events in combination

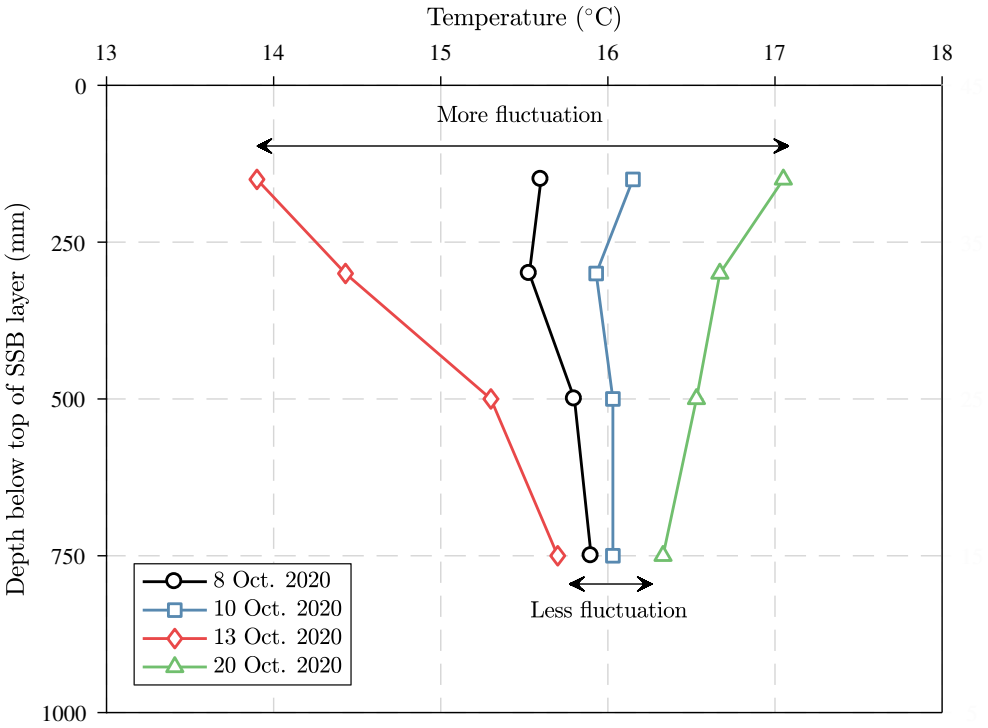

Figure 19: Temperature profiles within the formation layers at different times

with subdued air temperatures were observed to decrease the formation layers' temperatures, the extent of which was inversely related to depth. Therefore, the SSB layer showed the greatest variation in temperature over the observational period. Thus, it is concluded that the SSB layer showed the greatest variation in both suction and temperature and is the layer which experienced the greatest stress changes as a result of seasonal variations in rainfall and air temperature.

Field monitoring of suction beneath transportation infrastructure remains a time consuming and challenging task. However, recent developments in suction measurement apparatuses and techniques has allowed for the continuous monitoring thereof with minimal maintenance. The accuracy of these techniques still requires further research. The use of tensiometers for field suction measurement is a valuable technique but requires continuous maintenance. Data on the movement of ground water levels would be valuable and it is suggested that future work include the installation of piezometers in this regard. Suction conditions are expected to vary according to infrastructure type, location and climate and thus further research in this area is encouraged. It is recommended that future studies expand on the the number of monitored sites as well as the horizontal area monitored at each site, if possible. This could provide valuable data on the geospatial variation of soil suction along linear infrastructure such as railway lines. Furthermore, these studies may provide insight into any potential horizontal flow effects.

7. Acknowledgments

The authors gratefully acknowledge the assistance provided by the postgraduate students during the installation and maintenance of the equipment at the field testing site. The South African Weather Service is thanked for providing the rainfall data at the nearby Ermelo Airfield, which was used to compare and supplement the measurements taken on-site. The funding provided by Transnet Freight Rail towards the Chair in Railway Engineering is also gratefully acknowledged. Eskom is also thanked for allowing the site to be used for this research.

References

An, N., Hemmati, S., Cui, Y.J., 2017. Numerical analysis of soil volumetric water content and temperature variations in an embankment due to soil-atmosphere interaction. Computers and Geotechnics 83, 40–51. doi:10.1016/j.compgeo.2016.10.010.

ASTM, 2018. D2487-17: Standard Practice for Classification of Soils for Engineering Purposes (Unified Soil Classification System). ASTM International.

Blackmore, L., Clayton, C.R.I., Powrie, W., Priest, J.A., Otter, L., 2020. Saturation and its effect on the resilient modulus of a pavement formation material. Géotechnique 70, 292–302. doi:10.1680/jgeot.18.p.053.

Brown, S.F., 1996. Soil mechanics in pavement engineering. Géotechnique 46, 383–426. doi:10.1680/geot.1996.46.3.383.

Bulut, R., Leong, E.C., 2008. Indirect measurement of suction. Geotechnical and Geological Engineering 26, 633–644. doi:10.1007/s10706-008-9197-0.

Bulut, R., Lytton, R.L., Wray, W.K., 2001. Soil suction measurements by filter filter paper. Geotechnical Special Publication 115, 243–259. doi:10.1061/40592(270)14.

Chu, X., 2020. A review on the resilient response of unsaturated subgrade soils. Advances in Civil Engineering 2020. doi:10.1155/2020/7367484.

Cui, Y.J., Lamas-Lopez, F., Trinh, V.N., Calon, N., D'Aguiar, S.C., Dupla, J.C., Tang, A.M., Canou, J., Robinet, A., 2014. Investigation of interlayer soil behaviour by field monitoring. Transportation Geotechnics 1, 91–105. doi:10.1016/j.trgeo.2014.04.002.

Feng, M., Fredlund, D.G., Shuai, F., 2002. A laboratory study of the hysteresis of a thermal conductivity soil suction sensor. Geotechnical Testing Journal 25, 303–314.

Fredlund, D.G., 2019. Determination of unsaturated soil property functions for engineering practice, in: Jacobsz, S.W. (Ed.), Proceedings of the 17th African Regional Conference on Soil Mechanics and Geotechnical Engineering, Cape Town, South Africa. pp. 3–19.

Fredlund, D.G., Rahardjo, H., 1993. Soil mechanics for unsaturated soils. John Wiley & Sons, Inc., New York. doi:10.1002/9780470172759.

Gens, A., 2010. Soil-environment interactions in geotechnical engineering. Géotechnique 60, 3–74. doi:10.1680/geot.9.P.109.

Guan, Y., Fredlund, D.G., 1997. Use of the tensile strength of water for the direct measurement of high soil suction. Canadian Geotechnical Journal 34, 604–614. doi:10.1139/T97-014.

Harrison, B.A., Blight, G.E., 2000. A comparison of in-situ soil suction measurements, in: Rahardjo, H., Toll, D.G., Leong, E.C. (Eds.), Unsaturated Soils for Asia: Proceedings of the Asian Conference on Unsaturated Soils, Balkema, Singapore. pp. 281–285.

Houston, S., 2019. It is time to use unsaturated soil mechanics in routine geotechnical engineering practice. Journal of Geotechnical and Geoenvironmental Engineering 145. doi:10.1061/(ASCE)GT.1943-5606.0002044.

Jacobsz, S.W., 2018. Low cost tensiometers for geotechnical applications, in: Proceedings of the 9th International Conference on Physical Modelling in Geotechnics, CRC Press. pp. 305–310. doi:10.1201/9780429438660-40.

Karagoly, Y., Tripathy, S., Cleall, P.J., Mahdi, T., 2017. Suction measurements by a fixed-matrix porous ceramic disc sensor, in: Ng, C.W.W., Leung, A.K., Chiu, A.C.F., Zhou, C. (Eds.), Proceedings of the 7th International Conference on Unsaturated Soils, HKUST, Hong Kong. pp. 703–708.

Khoury, N.N., Zaman, M.M., 2004. Correlation between resilient modulus, moisture variation, and soil suction for subgrade soils. Transportation Research Record: Journal of the Transportation Research Board 1874, 99–107.

Kim, H., Prezzi, M., Salgado, R., 2017. Calibration of Whatman Grade 42 filter paper for soil suction measurement. Canadian Journal of Soil Science 97, 93–98. doi:10.1139/cjss-2016-0064.

Le Roux, P.F., Jacobsz, S.W., 2021. Performance of the tensiometer method for the determination of soil-water retention curves in various soils. Geotechnical Testing Journal 44. doi:10.1520/gtj20200196.

Leong, E.C., Abuel-Naga, H., 2018. Contribution of osmotic suction to shear strength of unsaturated high plasticity silty soil. Geomechanics for Energy and the Environment 15, 65–73. doi:10.1016/j.gete.2017.11.002.

Leong, E.C., Tripathy, S., Rahardjo, H., 2003. Total suction measurement of unsaturated soils with a device using the chilled-mirror dew-point technique. Géotechnique 53, 173–182. doi:10.1680/geot.2003.53.2.173.

Li, D., Hyslip, J., Sussman, T., Chrismer, S., 2016. Railway geotechnics. CRC Press.

Likos, W.J., Lu, N., 2002. Filter paper technique for measuring total soil suction. Transportation Research Record: Journal of the Transportation Research Board 1786, 120–128. doi:10.3141/1786-14.

Lourenço, S.D.N., Gallipoli, D., Toll, D.G., Augarde, C.E., Evans, F.D., 2011. A new procedure for the determination of soil-water retention curves by continuous drying using high-suction tensiometers. Canadian Geotechnical Journal 48, 327–335. doi:10.1139/T10-062.

Lu, N., 2020. Unsaturated soil mechanics: Fundamental challenges, breakthroughs, and opportunities. Journal of Geotechnical and Geoenvironmental Engineering 146. doi:10.1061/(asce)gt.1943-5606.0002233.

Lu, N., Likos, W.J., 2006. Suction stress characteristic curve for unsaturated soil. Journal of Geotechnical and Geoenvironmental Engineering 132, 131–142. doi:10.1061/(ASCE)1090-0241(2006)132:2(131).

Malazian, A., Hartsough, P., Kamai, T., Campbell, G.S., Cobos, D.R., Hopmans, J.W., 2011. Evaluation of MPS-1 soil water potential sensor. Journal of Hydrology 402, 126–134. doi:10.1016/j.jhydrol.2011.03.006.

Marinho, F.A.M., Oliveira, O.M., 2006. The filter paper method revisited. Geotechnical Testing Journal 29, 250–258. doi:10.1520/GTJ14125.

Marinho, F.A.M., da Silva Gomes, J.E., 2012. The effect of contact on the filter paper method for measuring soil suction. Geotechnical Testing Journal 35, 172–181. doi:10.1520/GTJ103571.

Matula, S., Bát'ková, K., Legese, W.L., 2016. Laboratory performance of five selected soil moisture sensors applying factory and own calibration equations for two soil media of different bulk density and salinity levels. Sensors 16. doi:10.3390/s16111912.

McCartney, J.S., Khosravi, A., 2013. Field-monitoring system for suction and temperature profiles under pavements. McCartney, John S.Khosravi, Ali 27. doi:10.1061/(ASCE)CF.1943-5509.0000362.

Mendes, J., Gallipoli, D., Toll, D.G., Augarde, C.E., 2008. A system for field measurement of suction using high capacity tensiometers, in: Unsaturated Soils: Advances in Geo-Engineering. Proceedings of the 1st European Conference on Unsaturated Soils, CRC Press/Balkema, Durham, UK. pp. 219–225. doi:10.1201/9780203884430.ch25.

Meter Group, Inc., 2017. Teros 21 User's Manual. Meter Group.

Meter Group, Inc., 2018. 5TM User's Manual. Meter Group.

Meter Group, Inc., 2020. WP4C User Manual. Meter Group.

Ng, C.W.W., Zhou, C., 2014. Cyclic behaviour of an unsaturated silt at various suctions and temperatures. Géotechnique 64, 709–720. doi:10.1680/geot.14.P.015.

Nichol, C., Smith, L., Beckie, R., 2003. Long-term measurement of matric suction using thermal conductivity sensors. Canadian Geotechnical Journal 40, 587–597. doi:10.1139/t03-012.

Parvin, N., Degré, A., 2016. Soil-specific calibration of capacitance sensors considering clay content and bulk density. Soil Research 54, 111–119. doi:10.1071/sr15036.

Puppala, A.J., Manosuthkij, T., Nazarian, S., Hoyos, L.R., 2011. Threshold moisture content and matric suction potentials in expansive clays prior to initiation of cracking in pavements. Canadian Geotechnical Journal 48, 519–531. doi:10.1139/t10-087.

Puppala, A.J., Manosuthkij, T., Nazarian, S., Hoyos, L.R., Chittoori, B., 2012. In situ matric suction and moisture content measurements in expansive clay during seasonal fluctuations. Geotechnical Testing Journal 35, 74–82. doi:10.1520/GTJ103597.

Qian, J., Chen, X., Ling, J., Li, J., 2021. Estimating the contribution of suction on the resilient modulus of subgrade soils using capillary saturation. Journal of Transportation Engineering, Part B: Pavements 147. doi:10.1061/JPEODX.0000244.

Van der Raadt, P.W., Fredlund, D.G., Clifton, A.W., Klassen, M.J., Jubien, W.E., 1987. Soil suction measurements at several sites in western Canada. Transportation Research Record 1137, 24–35.

Rahardjo, H., Kim, Y., Satyanaga, A., 2019. Role of unsaturated soil mechanics in geotechnical engineering. International Journal of Geo-Engineering 10. doi:10.1186/s40703-019-0104-8.

Ridley, A.M., 1993. The measurement of soil moisture suction. phdthesis. Imperial College of Science, Technology and Medicine.

Schulz-Poblete, M.V., Gräbe, P.J., Jacobsz, S.W., 2019. The influence of soil suctions on the deformation characteristics of railway formation materials. Transportation Geotechnics 18, 111–123. doi:10.1016/j.trgeo.2018.11.006.

Take, W.A., Bolton, M.D., 2003. Tensiometer saturation and the reliable measurement of soil suction. Géotechnique 54, 229–232. doi:10.1680/geot.2004.54.3.229.

Tarantino, A., Mongiovì, L., 2001. Experimental procedures and cavitation mechanisms in tensiometer measurements. Geotechnical and Geological Engineering 19, 189–210. doi:10.1023/A:1013174129126.

Tarantino, A., Mongiovì, L., 2003. Calibration of tensiometer for direct measurement of matric suction. Géotechnique 53, 137–141. doi:10.1680/geot.2003.53.1.137.

Tarantino, A., Ridley, A.M., Toll, D.G., 2008. Field measurement of suction, water content, and water permeability. Geotechnical and Geological Engineering 26, 751–782. doi:10.1007/s10706-008-9205-4.

Toll, D.G., Lourenço, S.D.N., Mendes, J., 2013. Advances in suction measurements using high suction tensiometers. Engineering Geology 165, 29–37. doi:10.1016/j.enggeo.2012.04.013.

Toll, D.G., Lourenço, S.D.N., Mendes, J., Gallipoli, D., Evans, F.D., Augarde, C.E., Cui, Y.J., Tang, A.M., Rojas, J.C., Pagano, L., Mancuso, C., Zingariello, C., Tarantino, A., 2011. Soil suction monitoring for landslides and slopes. Quarterly Journal of Engineering Geology and Hydrogeology 44, 23–33. doi:10.1144/1470-9236/09-010.

Toll, D.G., Mendes, J., Gallipoli, D., Glendinning, S., Hughes, P.N., 2012a. Investigating the impacts of climate change on slopes: field measurements. Geological Society, London, Engineering Geology Special Publications 26, 151–161. doi:10.1144/EGSP26.17.

Toll, D.G., Mendes, J., Hughes, P.N., Glendinning, S., Gallipoli, D., 2012b. Climate change and the role of unsaturated soil mechanics. Geotechnical Engineering Journal of the SEAGS & AGSSEA 43, 76–82.

Topp, G.C., 1980. Electromagnetic determination of soil water content: measurement in coaxial transmission lines. Water Resources Research 16, 574–582.

Transnet Freight Rail, 2006. Specification for Railway Earthworks S410. techreport. Transnet Freight Rail.

Tripathy, S., Al-Khyat, S., Cleall, P.J., Baille, W., Schanz, T., 2016. Soil suction measurement of unsaturated soils with a sensor using fixed-matrix porous ceramic discs. Indian Geotechnical Journal 46, 252–260. doi:10.1007/s40098-016-0200-z.

Varble, J.L., Chávez, J.L., 2011. Performance evaluation and calibration of soil water content and potential sensors for agricultural soils in eastern Colorado. Agricultural Water Management 101, 93–106. doi:10.1016/j.agwat.2011.09.007.

Xie, Y., Feng, S.j., Xiong, Y.l., Zhang, L.l., Ye, G.l., 2021. Coupled hydraulic-mechanical-air simulation of unsaturated railway embankment under rainfall and dynamic train load. Transportation Geotechnics 27. doi:10.1016/j.trgeo.2020.100463.

Zhang, N., Yu, X., Puppala, A.J., 2017. Design and evaluation of a moisture/suction TDR probe. Geotechnical Testing Journal 40, 762–775. doi:10.1520/GTJ20160139.

Zhou, C., Ng, C.W.W., 2016. Effects of temperature and suction on plastic deformation of unsaturated silt under cyclic loads. Journal of Materials in Civil Engineering 28. doi:10.1061/(ASCE)MT.1943-5533.0001685.